Rayleigh-Rayleigh chain

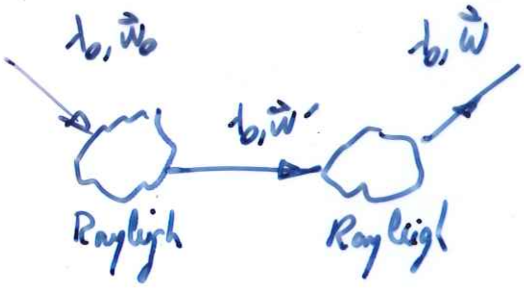

$$I^{(2)}_{(R,R)}(\vec{\omega},\lambda) = \frac{1-\mathrm{sgn}\,\eta}{2}\,\frac{1+\mathrm{sgn}\,\eta_0}{2}\,\frac{I_0}{|\eta_0|}\,\frac{\delta(\lambda-\lambda_0)}{\frac{\mu_0}{|\eta|}+\frac{\mu_0}{|\eta_0|}}\,\sigma^2$$

$$\Bigg\{ \int_0^{2\pi} d\varphi' \int_0^1 \frac{d\eta'}{\eta'} \frac{\left[1+(\vec{\omega}'\cdot\vec{\omega}_0^{(+)})^2\right]\left[1+(\vec{\omega}'\cdot\vec{\omega}^{(+)})^2\right]}{\frac{\mu_0}{|\eta|}+\frac{\mu_0}{\eta'}} \frac{F^2(\lambda_0,\vec{\omega}'\cdot\vec{\omega}_0^{(+)},Z)}{Z}\frac{F^2(\lambda_0,\vec{\omega}'\cdot\vec{\omega}^{(+)},Z)}{Z} +$$

$$\int_0^{2\pi} d\varphi' \int_0^1 \frac{d\eta'}{\eta'} \frac{\left[1+(\vec{\omega}'\cdot\vec{\omega}_0^{(-)})^2\right]\left[1+(\vec{\omega}'\cdot\vec{\omega}^{(-)})^2\right]}{\frac{\mu_0}{|\eta_0|}+\frac{\mu_0}{\eta'}} \frac{F^2(\lambda_0,\vec{\omega}'\cdot\vec{\omega}_0^{(-)},Z)}{Z}\frac{F^2(\lambda_0,\vec{\omega}'\cdot\vec{\omega}^{(-)},Z)}{Z} \Bigg\}$$

where

$$\vec{\omega}'\cdot\vec{\omega}_0^{(\pm)} = \pm\eta'\eta_0 + \sqrt{1-\eta'^2}\sqrt{1-\eta_0^2}\cos(\varphi'-\varphi_0)$$

$$\vec{\omega}'\cdot\vec{\omega}^{(\pm)} = \pm\eta'\eta + \sqrt{1-\eta'^2}\sqrt{1-\eta^2}\cos(\varphi'-\varphi)$$

- Discrete $(\lambda=\lambda_0)$
- Plane of symmetry
- Modifies also the coherent line

Rayleigh - Compton chain

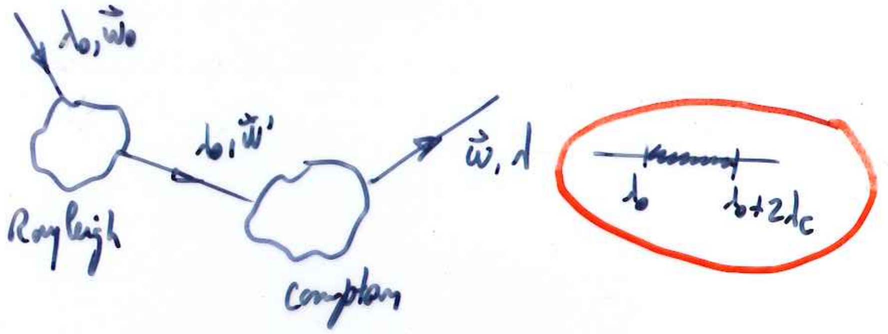

$$I^{(2)}_{(R,C)}(\vec{\omega}, \lambda) = \frac{1-\operatorname{sgn}\eta}{2}\,\frac{1+\operatorname{sgn}\eta_0}{2}\,\frac{I_0}{|\eta_0|\lambda_c}\,\frac{\sigma^2 K_{KN}(\lambda,\lambda_0)\, S(\lambda_0, a, Z)}{\frac{\mu}{|\eta|}+\frac{\mu_0}{|\eta_0|}}$$

$$\Bigg\{ \underset{(\alpha_2>\alpha_1)}{\int_{\alpha_1}^{\alpha_2}} \frac{d\eta'}{\eta'}\,\frac{1}{\frac{\mu_0}{\eta'}+\frac{\mu}{|\eta|}}\,\frac{1}{\sqrt{(1-\eta'^2)(1-\eta^2)-(a-\eta'\eta)^2}} \sum_{i=1}^{2}\left(1+(\vec{\omega}_0\cdot\vec{\omega}_i^{\,(+)})^2\right)\frac{F^2(\lambda_0, \vec{\omega}_0\cdot\vec{\omega}_i^{\,(+)}, Z)}{Z} +$$

$$\underset{(\beta_2>\beta_1)}{\int_{\beta_1}^{\beta_2}} \frac{d\eta'}{\eta'}\,\frac{1}{\frac{\mu_0}{|\eta_0|}+\frac{\mu_0}{\eta'}}\,\frac{1}{\sqrt{(1-\eta'^2)(1-\eta^2)-(a+\eta'\eta)^2}} \sum_{i=1}^{2}\left[1+(\vec{\omega}_0\cdot\vec{\omega}_i^{\,(-)})^2\right]\frac{F^2(\lambda_0, \vec{\omega}_0\cdot\vec{\omega}_i^{\,(-)}, Z)}{Z}\Bigg\}$$

where

$$a = 1+\frac{\lambda_0-\lambda}{\lambda_c}, \quad \varphi_1^{(\pm)} = \varphi + \arccos\frac{a\mp\eta'\eta}{\sqrt{(1-\eta'^2)(1-\eta^2)}}, \quad \varphi_2^{(\pm)} = \varphi + 2\pi - (\varphi_1^{(\pm)}-\varphi)$$

$$\vec{\omega}_0\cdot\vec{\omega}_i^{\,(\pm)} = \pm\eta_0\eta' + \sqrt{(1-\eta_0^2)(1-\eta'^2)}\,\cos(\varphi_i^{(\pm)})$$

$$\alpha_1 = \max\left(0, a\eta - \sqrt{(1-\eta^2)(1-a^2)}\right)$$

$$\alpha_2 = \min\left(1, a\eta + \sqrt{(1-\eta^2)(1-a^2)}\right)$$

$$\beta_1 = -\max\left(0, a\eta + \sqrt{(1-\eta^2)(1-a^2)}\right)$$

$$\beta_2 = -\min\left(-1, a\eta - \sqrt{(1-\eta^2)(1-a^2)}\right)$$

- Continuous $\lambda \in [\lambda_0, \lambda_0 + 2\lambda_c]$
- Modifies the Compton profile
- Overlaps the Compton-Rayleigh and Compton-Compton spectra
- May overlap other lines

Compton-Rayleigh chain

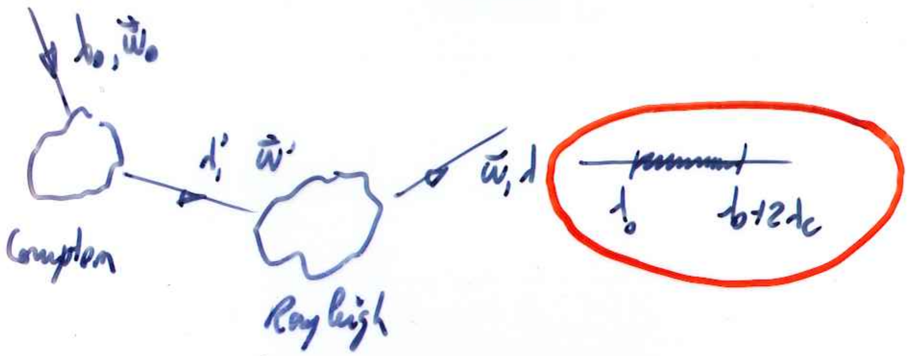

$$I^{(2)}_{(C,R)}(\vec{\omega},\lambda) = \frac{1-\operatorname{sgn}\gamma}{2}\,\frac{1+\operatorname{sgn}\gamma_0}{2}\,\frac{I_0}{|\gamma_0|\lambda_c}\,\frac{\sigma^c K_{KN}(\lambda,\lambda_0)\,S(\lambda_0,q,Z)}{\frac{\mu}{|\gamma|}+\frac{\mu_0}{|\gamma_0|}}$$

$$\left\{ \underset{(\alpha_2>\alpha_1)}{\int_{\alpha_1}^{\alpha_2}} \frac{d\gamma'}{\gamma'}\,\frac{1}{\frac{\mu}{|\gamma|}+\frac{\mu}{\gamma'}}\,\frac{1}{\sqrt{(1-\gamma'^2)(1-\gamma_0^2)-(a-\gamma'\gamma_0)^2}}\sum_{i=1}^{2}\left(1+(\vec{\omega}\cdot\vec{\omega}_i'^{(+)})^2\right)\frac{F^2(\lambda,\vec{\omega}\cdot\vec{\omega}_i'^{(+)},Z)}{Z} + \right.$$

$$\left. \underset{(\beta_2>\beta_1)}{\int_{\beta_1}^{\beta_2}} \frac{d\gamma'}{\gamma'}\,\frac{1}{\frac{\mu_0}{|\gamma_0|}+\frac{\mu}{\gamma'}}\,\frac{1}{\sqrt{(1-\gamma'^2)(1-\gamma_0^2)-(a+\gamma'\gamma_0)^2}}\sum_{i=1}^{2}\left(1+(\vec{\omega}\cdot\vec{\omega}_i'^{(-)})^2\right)\frac{F^2(\lambda,\vec{\omega}\cdot\vec{\omega}_i'^{(-)},Z)}{Z} \right\}$$

where $a = 1+\frac{\lambda_0-\lambda}{\lambda_c}$, $\varphi_1'^{(\pm)} = \arccos\frac{a\mp\gamma'\gamma_0}{\sqrt{(1-\gamma'^2)(1-\gamma_0^2)}}$, $\varphi_2'^{(\pm)} = 2\pi-\varphi_1'^{(\pm)}$

$$\vec{\omega}\cdot\vec{\omega}_i'^{(\pm)} = \pm\gamma\gamma' + \sqrt{(1-\gamma^2)(1-\gamma'^2)}\,\cos(\varphi_i'^{(\pm)}-\varphi)$$

$$\alpha_1 = \max\left(0,\ a\gamma_0-\sqrt{(1-\gamma_0^2)(1-a^2)}\right)$$

$$\alpha_2 = \min\left(1,\ a\gamma_0+\sqrt{(1-\gamma_0^2)(1-a^2)}\right)$$

$$\beta_1 = -\min\left(0,\ a\gamma_0+\sqrt{(1-\gamma_0^2)(1-a^2)}\right)$$

$$\beta_2 = -\max\left(-1,\ a\gamma_0-\sqrt{(1-\gamma_0^2)(1-a^2)}\right)$$

- Continuous $\lambda \in [\lambda_0, \lambda_0+2\lambda_c]$
- Modifies the Compton profile
- Overlaps the Rayleigh-Compton and Compton-Compton spectra
- May overlap other lines

Compton - Compton chain (detail)

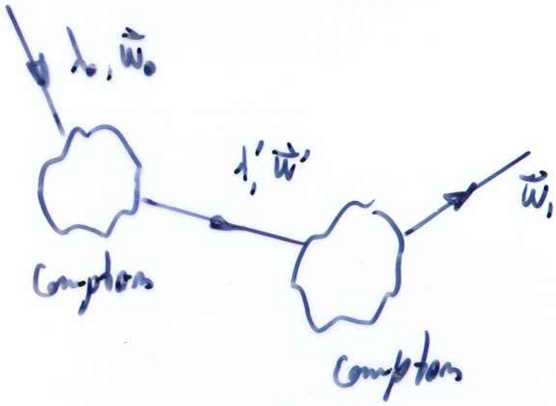

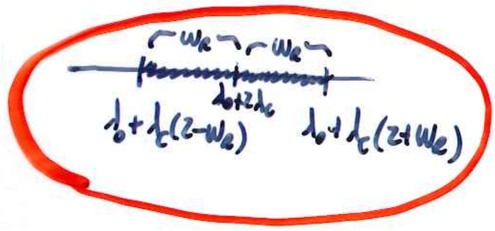

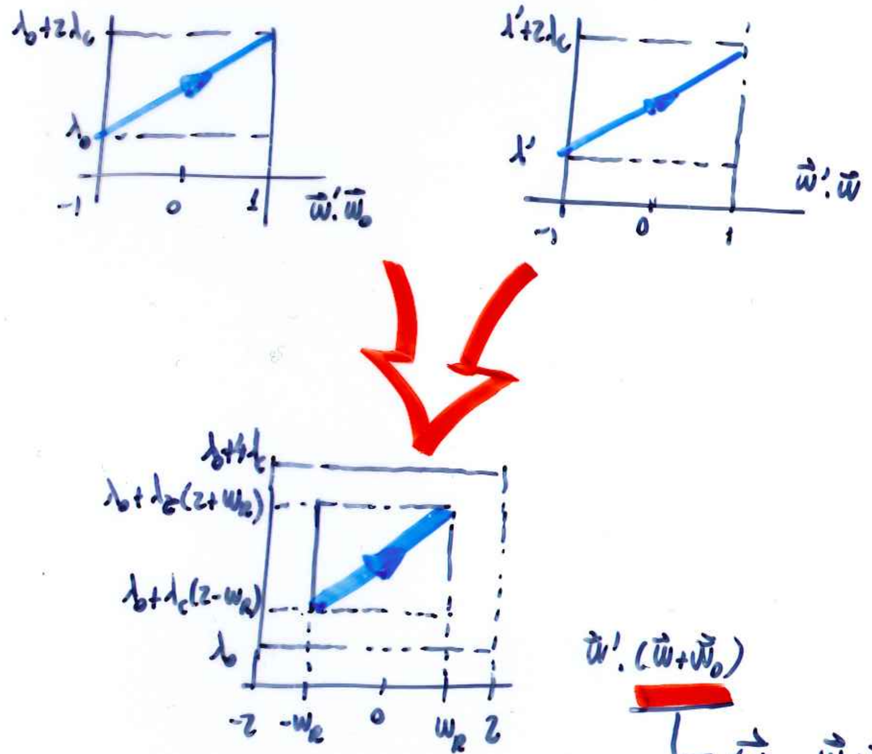

$\vec{\omega}'\cdot(\vec{\omega}+\vec{\omega}_0)$

$\vec{\omega}_R = \vec{\omega}+\vec{\omega}_0$

$\omega_R = \sqrt{2(1+\vec{\omega}\cdot\vec{\omega}_0)}$

$$I^{(2)}_{(S,C)}(\vec{\omega},\lambda) = \frac{1-\operatorname{sgn}\eta}{2}\,\frac{1-\operatorname{sgn}\eta_0}{2}\,\frac{I_0}{|\eta_0|}\,\frac{\sigma^2}{\frac{\mu}{|\eta|}+\frac{\mu_0}{|\eta_0|}}\int_0^\infty d\lambda' \int_{4\pi}\frac{d\vec{\omega}'}{|\eta'|}\,K_{KN}(\lambda,\lambda')\,K_{KN}(\lambda',\lambda_0)$$

$$S(\lambda', \vec{\omega}\cdot\vec{\omega}', z)\,S(\lambda_0, \vec{\omega}'\cdot\vec{\omega}_0, z)\,\delta\left(\lambda_c(1-\vec{\omega}'\cdot\vec{\omega}_0)+\lambda_0-\lambda'\right)\delta\left(\lambda_c(1-\vec{\omega}'\cdot\vec{\omega})+\lambda'-\lambda\right)$$

$$\left\{\frac{1+\operatorname{sgn}\eta'}{2}\,\frac{1}{\frac{\mu}{|\eta|}+\frac{\mu'}{|\eta'|}} + \frac{1-\operatorname{sgn}\eta'}{2}\,\frac{1}{\frac{\mu_0}{|\eta_0|}+\frac{\mu'}{|\eta'|}}\right\}$$

Integration over λ' and Dirac-δ properties give

$$I^{(2)}_{(S,C)}(\vec{\omega},\lambda) = \frac{1-\operatorname{sgn}\gamma}{2}\,\frac{1+\operatorname{sgn}\gamma_0}{2}\,\frac{I_0}{|\gamma_0|\lambda_c}\,\frac{\sigma^2}{\frac{\mu}{|\gamma|}+\frac{\mu_0}{|\gamma_0|}}\int_{4\pi}\frac{d\vec{\omega}'}{|\gamma'|}K_{KN}(\lambda,\tilde{\lambda})K_{KN}(\tilde{\lambda},\lambda_0)$$

$$S(\tilde{\lambda},\vec{\omega}\cdot\vec{\omega}';z)\,S(\lambda_0,\vec{\omega}'\cdot\vec{\omega}_0,z)\,\delta\left(2-\vec{\omega}'\cdot\vec{\omega}_R+\frac{\lambda_0-\lambda}{\lambda_c}\right)\left\{\frac{1+\operatorname{sgn}\gamma'}{2}\,\frac{1}{\frac{\mu}{|\gamma|}+\frac{\mu(\tilde{\lambda})}{|\gamma'|}}+\frac{1-\operatorname{sgn}\gamma'}{2}\,\frac{1}{\frac{\mu_0}{|\gamma_0|}+\frac{\mu(\tilde{\lambda})}{|\gamma'|}}\right\}$$

where $\tilde{\lambda} = \lambda_0+\lambda_c(1-\vec{\omega}'\cdot\vec{\omega}_0)$

The δ-function can be written as

$$\delta\left(2-\vec{\omega}'\cdot\vec{\omega}_R+\frac{\lambda_0-\lambda}{\lambda_c}\right)=$$

$$=\delta\left(a-\omega_R\left(\gamma'\gamma_R+\sqrt{(1-\gamma'^2)(1-\gamma_R^2)}\cos(\varphi'-\varphi_R)\right)\right)$$

where

$$a=2+\frac{\lambda_0-\lambda}{\lambda_c}\,,\quad \gamma_R=\frac{\gamma+\gamma_0}{\omega_R}\,,\quad \varphi_R=\arccos\left(\frac{\sqrt{1-\gamma_0^2}+\sqrt{1-\gamma^2}\cos\varphi}{\sqrt{\omega_R^2-(\gamma_0+\gamma)^2}}\right)$$

for $\boxed{\omega_R\neq 0}$ we have

$$\delta\left(2-\vec{\omega}'\cdot\vec{\omega}_R+\frac{\lambda_0-\lambda}{\lambda_c}\right)=$$

$$=\frac{1}{\omega_R}\,\delta\left(\alpha-\gamma'\gamma_R-\sqrt{1-\gamma'^2}\sqrt{1-\gamma_R^2}\cos(\varphi'-\varphi_R)\right)$$

where $\alpha=\dfrac{a}{\omega_R}$.

The δ-function depends on γ' <u>and</u> φ'. Is it possible to separate it into a part in φ' and a part in γ'?

The condition into the δ satisfies for some values of $\cos(\varphi'-\varphi_R)$. Since the cosine function is defined in $[-1,1]$, that condition is equivalent to

$$\frac{(\alpha-\gamma'\gamma_R)^2}{(1-\gamma'^2)(1-\gamma_R^2)}\leq 1 \qquad (*)$$

Condition (C.1) can be written as

$$(\alpha-\eta'\eta_R)^2 \le (1-\eta'^2)(1-\eta_R^2)$$

or

$$(\alpha^2+\eta_R-1) - 2\alpha\eta_R\eta' + \eta'^2 \le 0 \qquad \text{(C.2)}$$

which can be expressed as

$$(\eta'-\eta_1')(\eta'-\eta_2') \le 0 \qquad (\eta_1' \text{ and } \eta_2' \text{ are the roots of (C.2)})$$

$$\eta_{1,2}' = \alpha\eta_R \pm \sqrt{(1-\eta_R^2)(1-\alpha^2)}$$

Then we have that η' satisfies

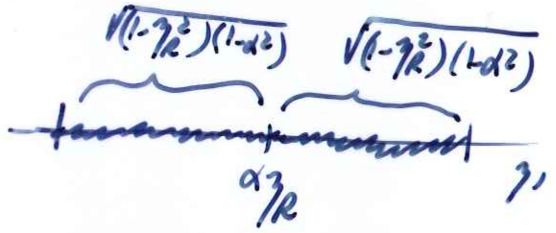

We will use also the δ-function property $\delta[g(x)] = \sum_n \frac{\delta(x-x_n)}{|g'(x_n)|}$, $g(x_n)=0, g'(x_n)\neq 0$ to extract the φ' dependence of the δ

$$\delta\left(\alpha-\eta'\eta_R-\sqrt{1-\eta'^2}\sqrt{1-\eta_R^2}\cos(\varphi'-\varphi_R)\right) = \sum_{i=1}^{2} \frac{\delta(\varphi'-\varphi_i')}{|g'(\varphi_i')|}$$

$$= \sum_{i=1}^{2} \frac{\delta(\varphi'-\varphi_i')}{\sqrt{(1-\eta'^2)(1-\eta_R^2)-(\alpha-\eta'\eta_R)^2}}$$

where $\varphi_1 = \varphi_R + \arccos\left(\frac{\alpha-\eta'\eta_R}{\sqrt{(1-\eta'^2)(1-\eta_R^2)}}\right)$

$\varphi_2 = 2\pi + \varphi_R - (\varphi_1-\varphi_R)$

Finally

$$\delta\left(z - \vec{w}'\cdot\vec{w}_R + \frac{\lambda_0-\lambda}{\lambda_c}\right) = \frac{1}{w_R}\frac{\delta(\varphi'-\varphi_1')+\delta(\varphi'-\varphi_2')}{\sqrt{(1-\gamma'^2)(1-\gamma_R^2)-(\alpha-\gamma'\gamma_R)^2}}$$

$$\left\{\mathcal{U}\left(\gamma'-(\alpha\gamma_R-\sqrt{(1-\gamma_R^2)(1-\alpha^2)}\right)-\mathcal{U}\left(\gamma'-(\alpha\gamma_R+\sqrt{(1-\gamma_R^2)(1-\alpha^2)})\right)\right\}$$

By substituting in the last expression of $I^{(2)}_{(SC)}$ we obtain after some algebra

$$I^{(2)}_{(SC)}(\vec{w},\lambda) = \frac{1-\mathrm{sgn}\,\gamma}{2}\,\frac{1+\mathrm{sgn}\,\gamma_0}{2}\,\frac{I_0}{|\gamma_0|\lambda_c w_R}\,\frac{\sigma^2}{\frac{\mu}{|\gamma|}+\frac{\mu_0}{|\gamma_0|}}$$

$$\left\{\underset{(\alpha_2>\alpha_1)}{\int_{\alpha_1}^{\alpha_2}}\frac{d\gamma'}{\gamma'}\frac{1}{\sqrt{(1-\gamma'^2)(1-\gamma_R^2)-(\alpha-\gamma'\gamma_R)^2}}\sum_{i=1}^{2}\frac{K_{KN}(\lambda,\tilde{\lambda}_i^{(+)})K_{KN}(\tilde{\lambda}_i^{(+)},\lambda_0)\,S(\tilde{\lambda}_i^{(+)},\vec{w}\cdot\vec{w}_i^{(+)},z)\,S(\lambda_0,\vec{w}_0\cdot\vec{w}_i^{(+)},z)}{\frac{\mu}{|\gamma|}+\frac{\mu(\tilde{\lambda}_i^{(+)})}{\gamma'}}\right. +$$

$$\left.+\underset{(\beta_2>\beta_1)}{\int_{\beta_1}^{\beta_2}}\frac{d\gamma'}{\gamma'}\frac{1}{\sqrt{(1-\gamma'^2)(1-\gamma_R^2)-(\alpha+\gamma'\gamma_R)^2}}\sum_{i=1}^{2}\frac{K_{KN}(\lambda,\tilde{\lambda}_i^{(-)})K_{KN}(\tilde{\lambda}_i^{(-)},\lambda_0)\,S(\tilde{\lambda}_i^{(-)},\vec{w}\cdot\vec{w}_i^{(-)},z)\,S(\lambda_0,\vec{w}_0\cdot\vec{w}_i^{(-)},z)}{\frac{\mu_0}{|\gamma_0|}+\frac{\mu(\tilde{\lambda}_i^{(-)})}{|\gamma'|}}\right\}$$

where $\tilde{\lambda}_i^{(\pm)} = \lambda_0 + \lambda_c\left(1-\vec{w}'\cdot\vec{w}_{0i}^{(\pm)}\right)$

$$\vec{w}'\cdot\vec{w}_{0i}^{(\pm)} = \pm\gamma'\gamma_0 + \sqrt{1-\gamma'^2}\sqrt{1-\gamma_0^2}\cos(\varphi_i^{(\pm)})$$

$$\alpha_1 = \max\left(0, \alpha\gamma_R - \sqrt{(1-\alpha^2)(1-\gamma_R^2)}\right)$$

$$\alpha_2 = \min\left(1, \alpha\gamma_R + \sqrt{(1-\alpha^2)(1-\gamma_R^2)}\right)$$

$$\beta_1 = -\min\left(0, \alpha\gamma_R + \sqrt{(1-\alpha^2)(1-\gamma_R^2)}\right)$$

$$\beta_2 = -\max\left(-1, \alpha\gamma_R - \sqrt{(1-\alpha^2)(1-\gamma_R^2)}\right)$$

- Continuous $\lambda \in \left[\lambda_0+\lambda_c(z-w_R), \lambda_0+\lambda_c(z+w_R)\right]$
- Overlaps the Compton-Rayleigh and the Rayleigh-Compton chains
- Modifies the Compton profile
- May overlap other lines

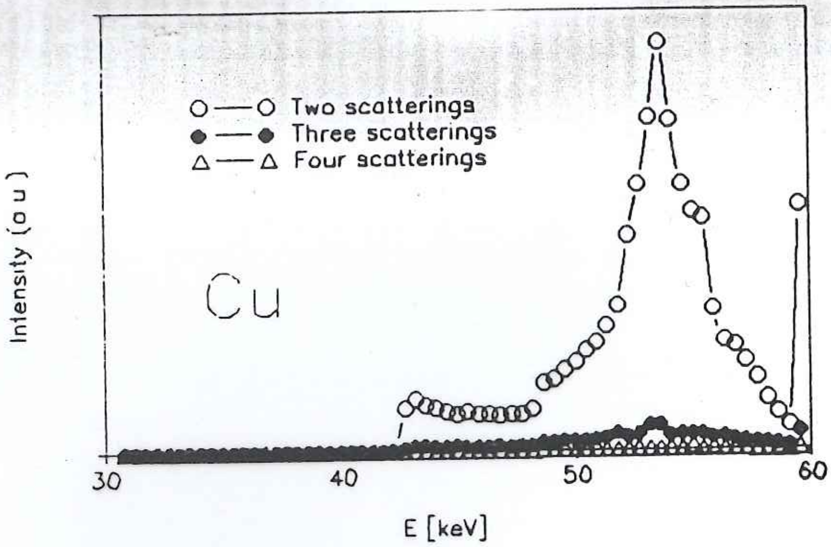

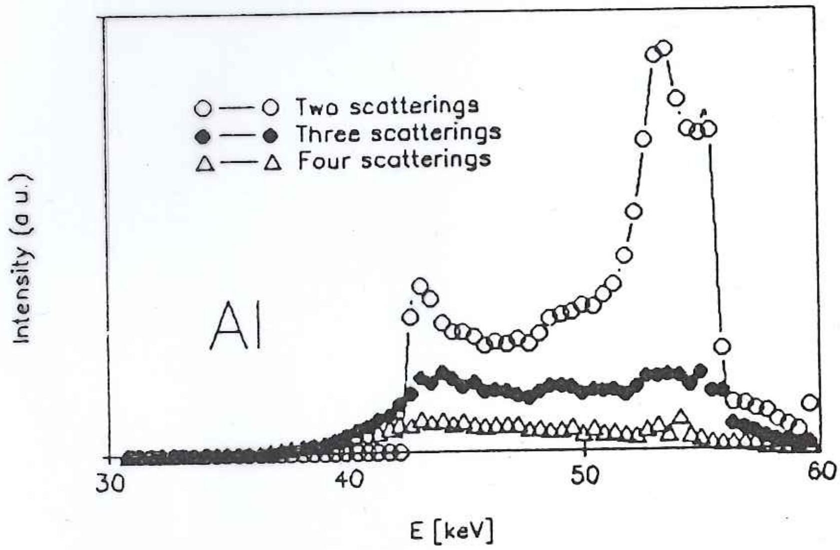

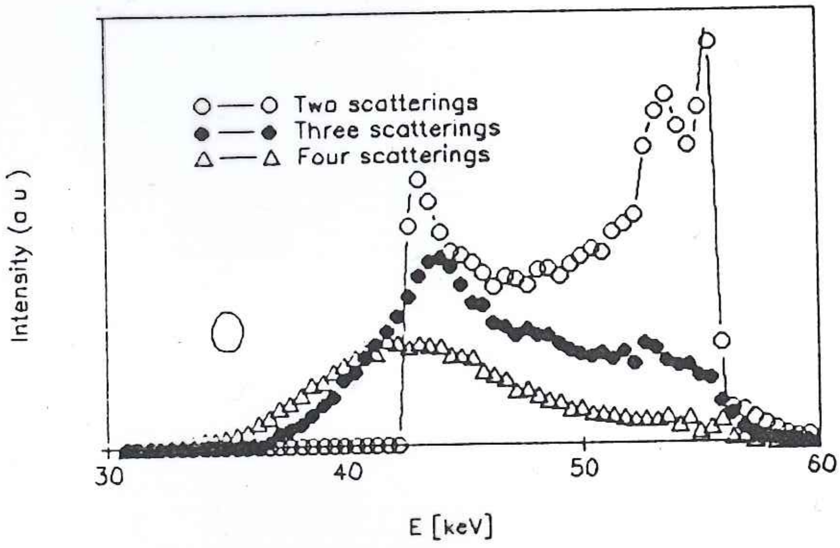

Influence of Higher-orders of scattering

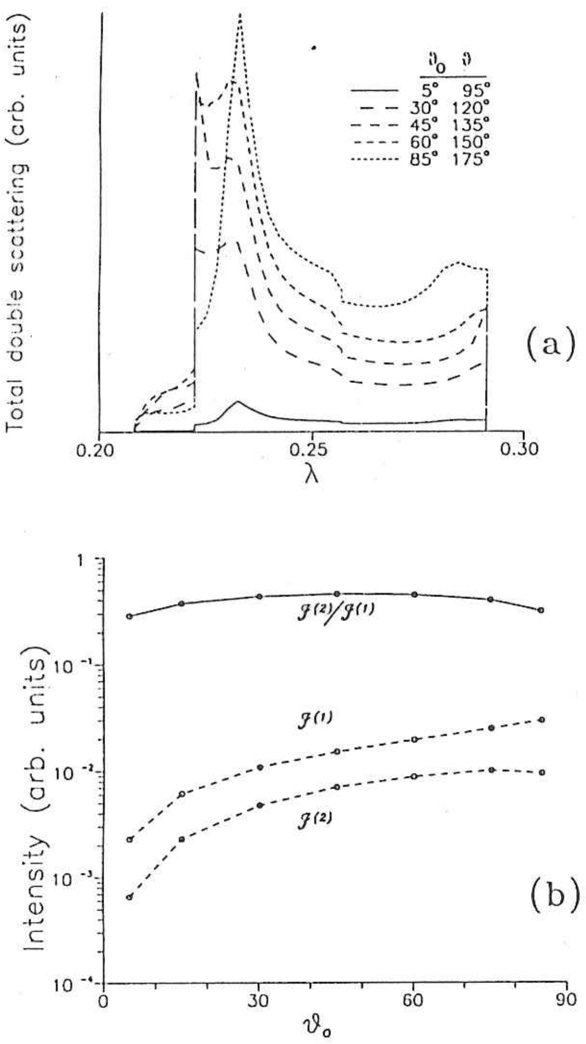

FIG. 7. (a) Double-scattering spectra of Al for a fixed scattering angle of 90° and $E_0=59.54$ keV. The incidence (take-off) polar angles are tilted in the scattering plane (maintaining χ unchanged) with values 5° (95°), 30° (120°), 45°(135°), 60° (150°), and 85° (175°), showing the change of the absorption for different geometrical situations. (b) Integrated intensities of single and double scattering as a function of the incidence polar angle for the cases explained above. With a solid line is plotted, in the same graph, the double- to single-intensity ratio which has a maximum near 45°.

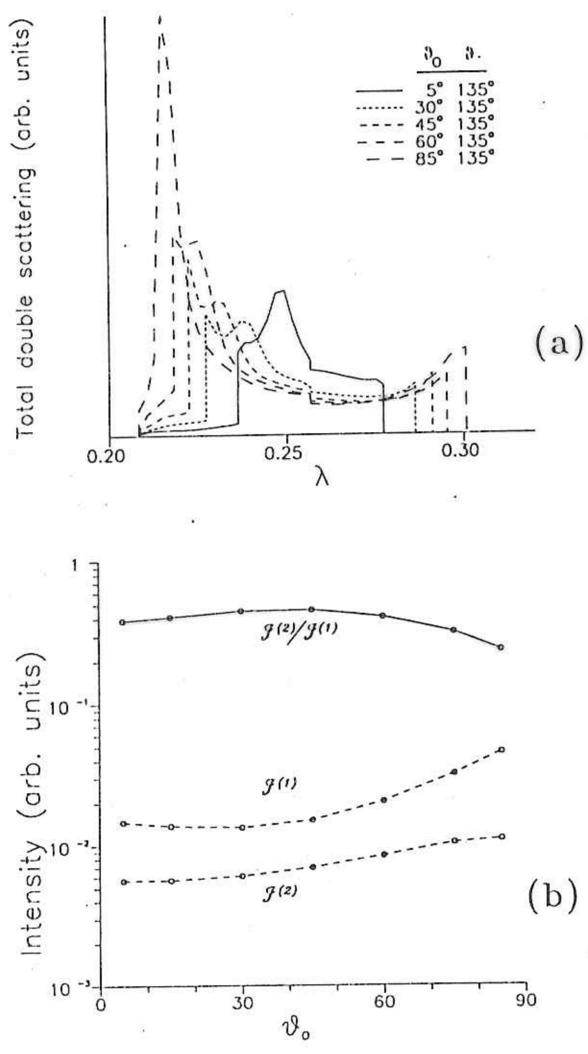

FIG. 8. (a) Total double-scattering spectra of Al, with fixed take-off angle of 135° and $E_0=59.54$ keV. The incidence polar angle is tilted in the same scattering angle plane with values 5°, 30°, 45°, 60°, and 85°. (b) Single and double scattering as a function of the incidence polar angle for Al, with fixed take-off polar angle of 135° and $E_0=59.54$ keV. The double- to single-intensity ratio is plotted in the same graph as a solid line.

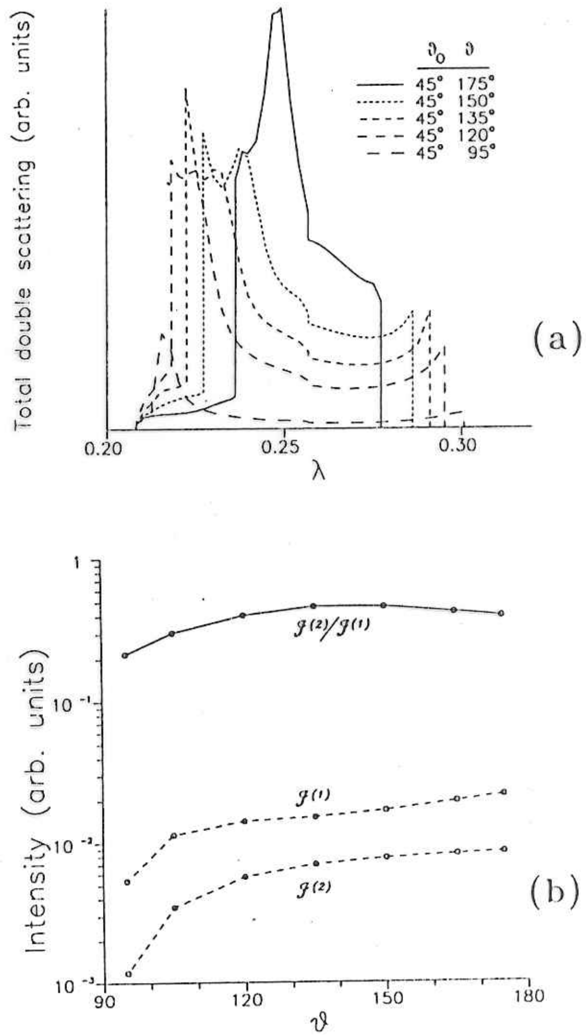

FIG. 9. (a) Total double-scattering spectra of Al, with fixed incidence polar angle of 45° and $E_0=59.54$ keV. The take-off polar angle is tilted in the same scattering plane with values 175°, 150°, 135°, 120°, and 95°. (b) Single and double scattering as a function of the take-off polar angle of Al, with fixed incidence polar angle of 45° and $E_0=59.54$ keV. The double- to single-intensity ratio is plotted in the same graph as a solid line.

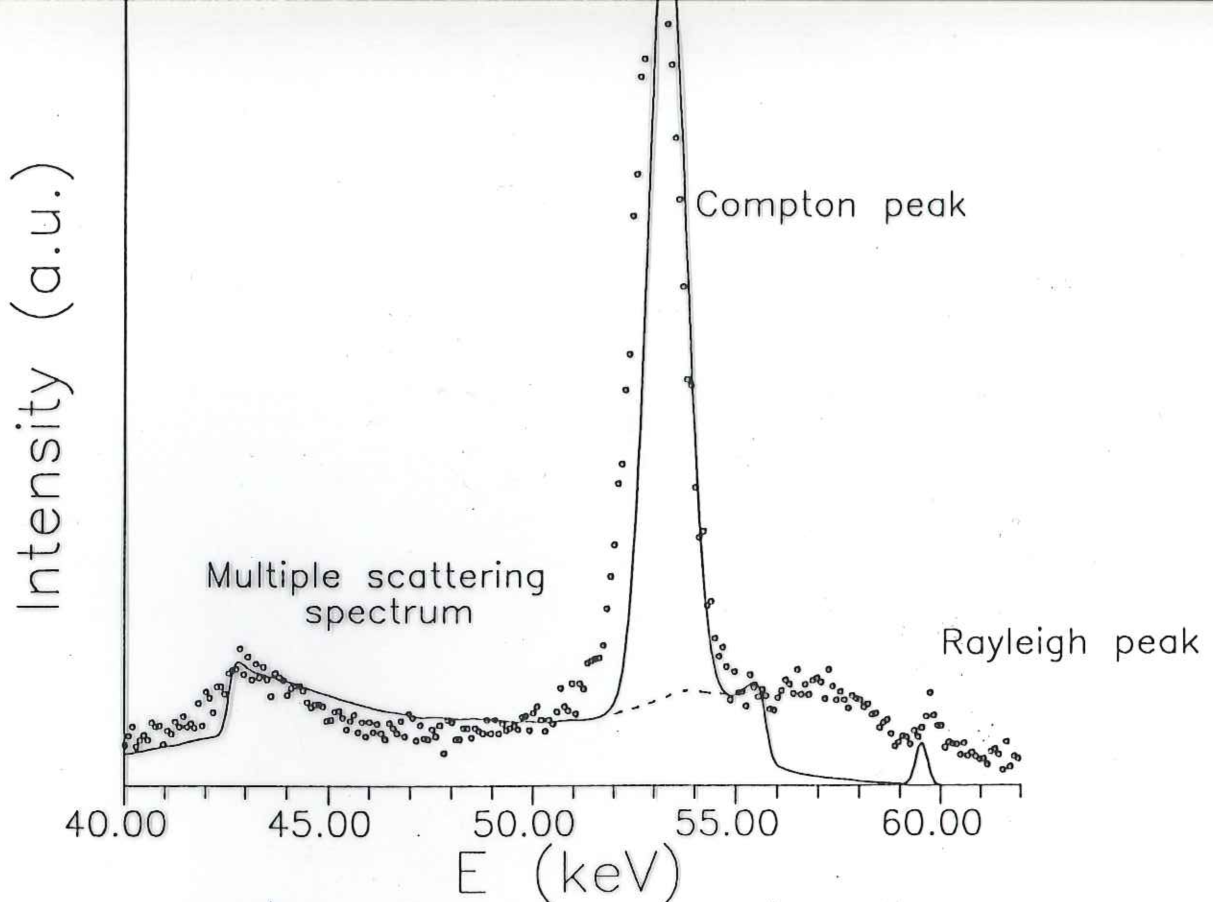

FERNANDEZ, PHYS. REV. A 44, 4232 (1991)

TARTARI et al., X-RAY SPECTROM. 22, 323 (1993)

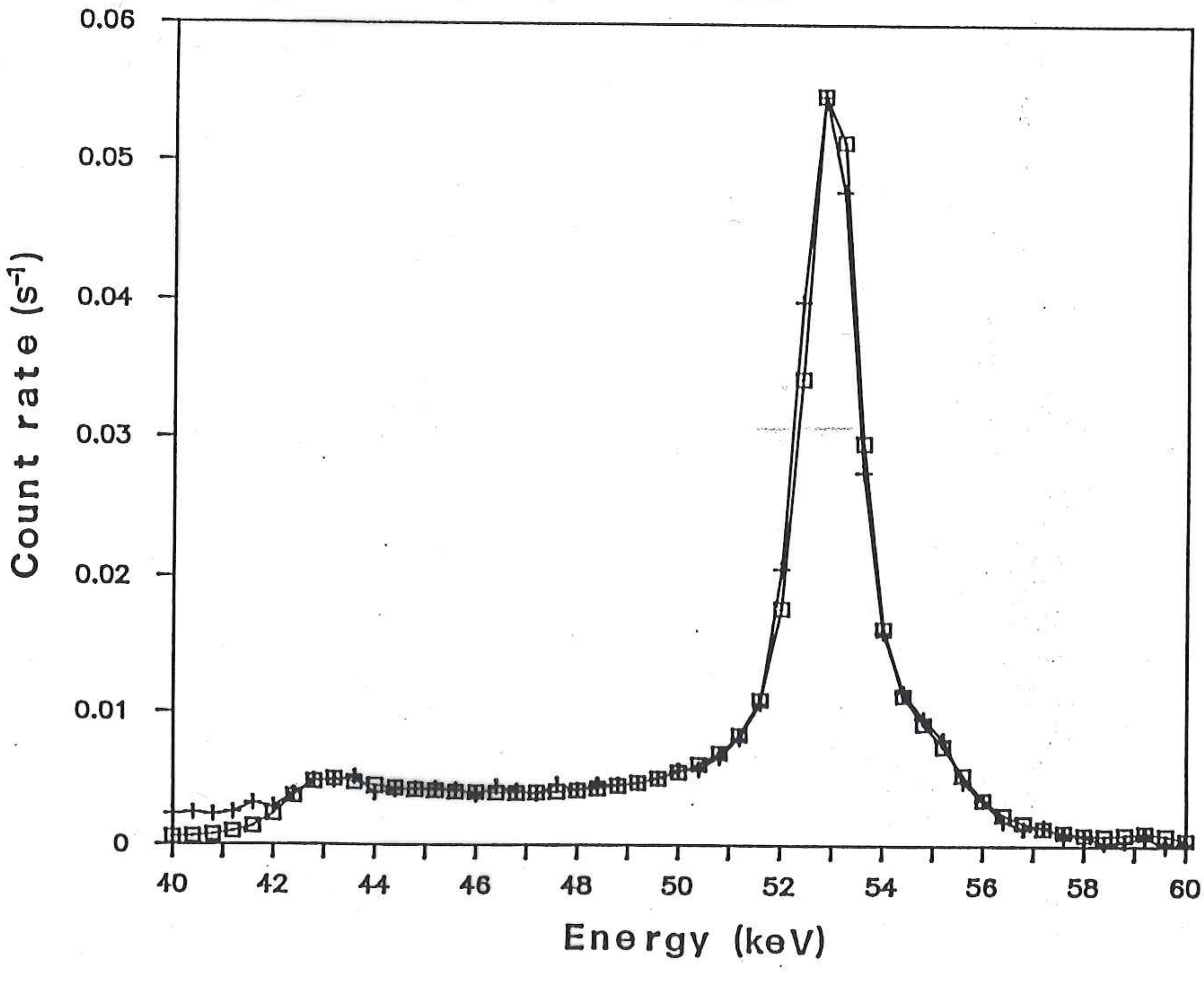

POLYCHROMATIC EXCITATION ON A BIOLOGICAL TISSUE

A. TARTARI et al. Phys. Med. Biol. 39, 219-230 (1994).

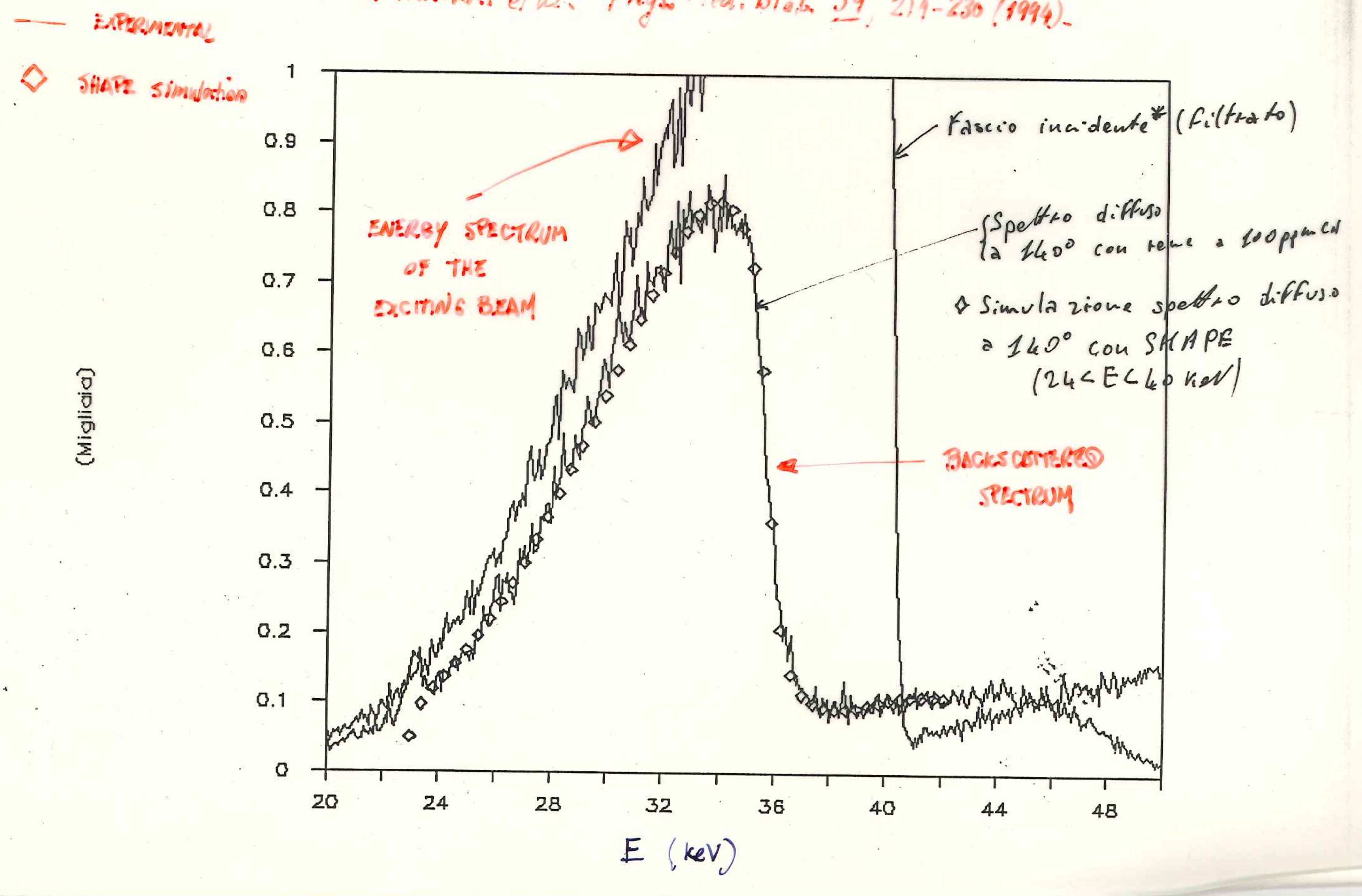

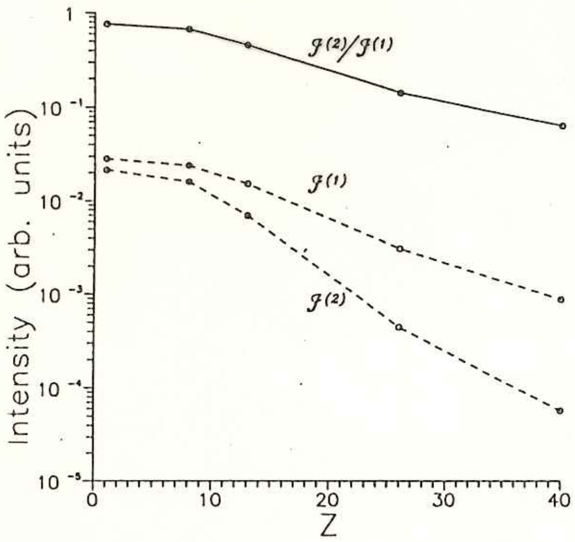

FIG. 4. The single- and double-scattering integrated intensi-
ies describing the overall contribution of the corresponding or-
er of scattering. Here they are plotted as a function of the
tomic number Z of the target for some representative elements
I,O,Al,Fe,Zr), polar angles of $\vartheta_0=45°$ and $\vartheta=135°$ and an ex-
itation of 59.54 keV. The double- to single-intensity ratio
$^{(2)}/\mathcal{J}^{(1)}$ that gives the importance of the continuous second-
rder (Compton-Compton, Rayleigh-Compton, and Compton-
ayleigh) terms relative to the intensity of the Compton peak is
lotted with a solid line.

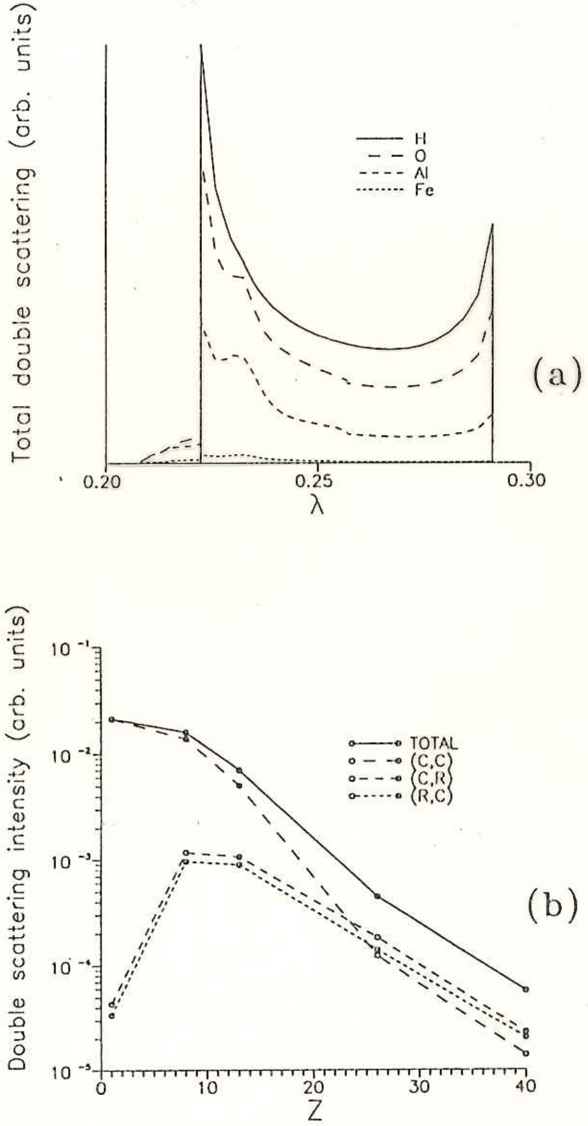

FIG. 5. (a) Total double-scattering wavelength spectra for some elements from H to Fe. The intensity of the double scattering is substantially greater for lighter elements. For heavier elements the Compton-Rayleigh and Rayleigh-Compton mixed contributions become more important. (b) Partial double-scattering intensities as a function of the atomic number Z. The Compton-Compton, Compton-Rayleigh, and Rayleigh-Compton continuous contributions are plotted as a dashed line. The total double scattering is plotted with a solid line. $\vartheta_0=45°$, $\vartheta=135°$, and the energy is 59.54 keV.

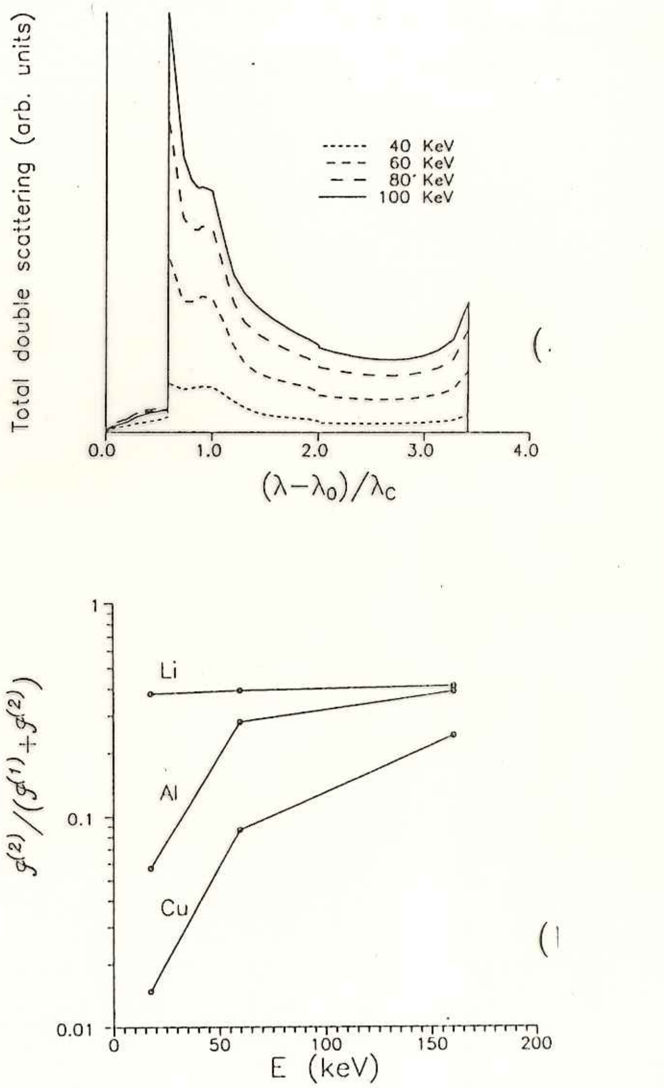

FIG. 6. (a) Total double scattering in Al as a function of the ratio $(\lambda-\lambda_0)/\lambda_C$ for several incidence energies E_0. The incidence and take-off angles are 45° and 135°, respectively. The double scattering importance $\mathcal{R}_{double}$ for Li, Al, and Cu as a function of the incidence energy E_0. Three values of E_0 were used in the calculations (17.5, 60, and 160 keV) that approximately correspond to the energy of some excitation lines reported frequently in the literature (Mo $K\alpha$, ^{241}Am and ^{123}Tc). cidence is normal and take-off is 150°. These values may be compared to Monte Carlo simulations performed in similar conditions (Ref. [42]).

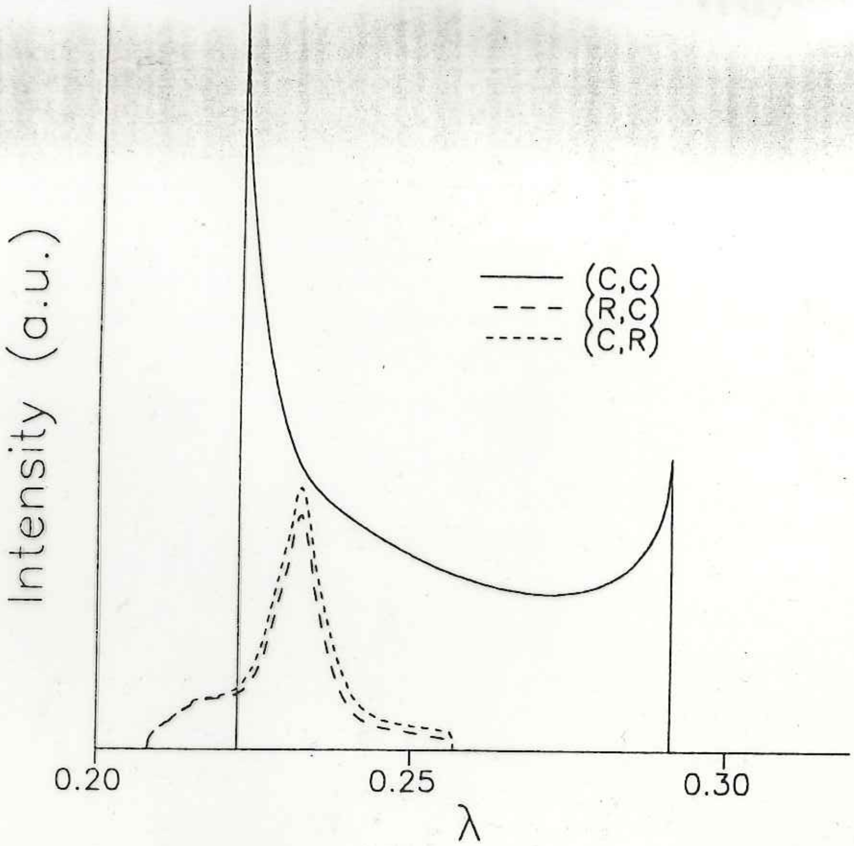

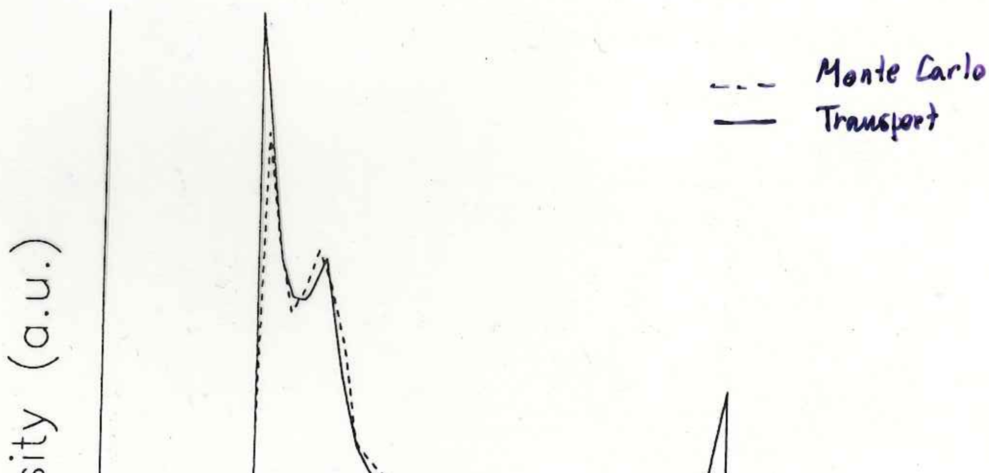

Comparison with Monte Carlo (second-order only)